



Semnan University

# Mechanics of Advanced Composite Structures

Journal homepage: <https://macs.semnan.ac.ir/>

ISSN: 2423-7043



## Research Article

# Effect of Ceramic Boron Carbide Particles Addition on the Mechanical and Microstructural Characteristics of Al7020 Alloy Composites

Shrishail Basappa Angadi <sup>a\*</sup>, Santosh Kumar <sup>b</sup>, Madeva Nagaral <sup>c</sup>, Virupaxi Auardi <sup>d</sup>, Balaraj Valukula <sup>e</sup>

<sup>a</sup> Department of Mechanical Engineering, KLE Technological University, Dr. M. S. Sheshgiri College of Engineering & Technology, Belagavi, 590008, Karnataka, India

<sup>b</sup> Department of Industrial and Production Engineering, The National Institute of Engineering, Mysuru, 570008, Karnataka, India

<sup>c</sup> Aircraft Research and Design Centre, Hindustan Aeronautics Limited, Bangalore, 560037, Karnataka, India

<sup>d</sup> Department of Mechanical Engineering, Siddaganga Institute of Technology, Tumkur, 572103, Karnataka, India

<sup>e</sup> Department of Mechanical Engineering, Rao Bahadur Y. Mahabaleswarappa Engineering College, Ballari, 583104, Karnataka, India

b

## ARTICLE INFO

## ABSTRACT

### Article history:

Received: 2023-10-19

Revised: 2024-03-22

Accepted: 2024-05-12

### Keywords:

Metal Matrix Composites;

Microstructure;

Tensile Properties;

Fracture Strength.

The aerospace and automotive engineering industries are seeing a growing need for materials that are both lightweight and very durable. This increased demand has prompted the development of innovative metal matrix composites based on aluminum. The current study aimed at developing and characterization Al7020 metal matrix composites by reinforcing micro boron carbide particles, Al7020/B<sub>4</sub>C MMCs are fabricated by stir casting method by varying the boron carbide particles in wt.% (0, 2, 4, 6, and 8wt. %). Lastly, the prepared samples were subjected to tensile, compression, hardness, and fracture toughness tests to evaluate the impact of B<sub>4</sub>C particles on density, mechanical, and microstructural parameters. By incorporating B<sub>4</sub>C particles into the Al7020 alloy, the experimental results demonstrated that metal matrix composites exhibited enhanced ultimate tensile strength, yield strength, hardness, and compression strength. In addition, the lowest density, highest toughness, and superior micrograph were observed in Al7020/B<sub>4</sub>C MMCs with 8 wt. % reinforcement of B<sub>4</sub>C particles with a minor decrease in elongation.

© 2025 The Author(s). Mechanics of Advanced Composite Structures published by Semnan University Press.

This is an open access article under the CC-BY 4.0 license. (<https://creativecommons.org/licenses/by/4.0/>)

## 1. Introduction

Metal matrix composites (MMCs) are extensively utilized across various industries owing to their advantageous characteristics, such as a superior modulus, a remarkable strength-to-weight ratio, exceptional thermal conductivity, and mild thermal expansion [1-3]. MMCs exhibit the metallic characteristics of the matrix, such as

ductility and toughness, as well as the features of ceramic reinforcements, including strength and high modulus [4-7]. The combination of these qualities results in exceptional shear, tensile, and compression resistance, as well as high-temperature capabilities [8-11]. Aluminum alloys are highly favored as matrix materials in various metal alloys due to their lightweight

\* Corresponding author.

E-mail address: [madev.nagaral@gmail.com](mailto:madev.nagaral@gmail.com)

Cite this article as:

Shrishail Basappa angadi et al., 2025. Title of article. *Mechanics of Advanced Composite Structures*, 12(1), pp. xx-xx

<https://doi.org/10.22075/MACS.2024.39315.2050>

nature, excellent thermal and electrical conductivity, and impressive capacity to resist corrosion [12–15].

Lightweight materials are in high demand because of their strength, which prompted the creation of innovative aluminum-based MMCs using many techniques [16]. Various types of reinforcements and processing processes were reviewed by Kumar et al. [17], who studied the manufacture of MMCs during the last 50 years. Typical properties of the reinforcing phase include low density, excellent chemical and mechanical compatibility, high thermal stability, compression strength, and Young's modulus [18]. When associated with other fabrication techniques like powder metallurgy, stir casting is the most popular for producing composites since it is both inexpensive and well-suited for mass manufacturing of machine components. Producing particulate-reinforced MMCs is a common application of the stir-casting process.

Research on aluminum alloys with SiC, B<sub>4</sub>C, and MoS<sub>2</sub> particles has been conducted by multiple researchers. Their findings indicate that the addition of reinforcement particles improves the physical and mechanical properties of the alloy [19, 20]. Researchers Ashok et al. [21] looked at the compressive and tensile strengths of stir-cast Al6061 MMCs reinforced with B<sub>4</sub>C. Their findings indicate that the mechanical qualities are enhanced by including 9 weight percent B<sub>4</sub>C particles. Satheesh and Pugazhavadivu [22] conducted a study on the physical and mechanical characteristics of Al6061. They investigated the effects of adding SiC (mesh size 220) and coconut shell ash (40–80 μm size) to the Al6061 alloy. The MMCs (Metal Matrix Composites) were created using the stir-casting method. The best MMC had a hardness of 100 VHN and a strength of 200 MPa. Madeva et al. [23] conducted a study where they created and analyzed the microstructure and mechanical properties of Al6061, Al6061 + 9 wt. % SiC, and Al6061 + 9 wt. % graphite particle metal matrix composites (MMCs) using liquid metallurgy. The Al6061 + 9 wt. % SiC MMCs exhibited a 25.32% enhancement in ultimate strength when compared to the Al6061.

Many researchers in the past studied friction stir processing of AA7020 aluminum alloy, and the effect of rotational and translation speed was examined on the mechanical properties and microstructure of AA-7020 aluminum alloy Atabak Rahimzadehikhechi [24]. Zeeshan et al. [25] conducted an empirical study on copper alloy with graphite-ZrO<sub>2</sub> composites. The study focused on determining the ideal process parameters and investigating the properties of these composites. Akbar Heidarzadeh et al. [26] employed surface response methods to forecast

and enhance the tensile characteristics of friction stir welded AA7020. The findings demonstrated that as the heat input increased, the tensile strength of the joints initially rose to a peak value before declining, but the elongation of the joints consistently increased. Samuel et al. [27] discussed a major challenge in the processing of aluminum alloy –TiB<sub>2</sub> composites, mainly focused on the in-situ processing method.

Cun-zhu Nie, et al. [28] conducted research on the reinforcement of Al2024 aluminum matrix composites with boron carbide particles. The samples were effectively manufactured using hot extrusion technology. Chaitra H. M. et al. [29] conducted a study on the reinforcement of aluminum 7075 (Al 7075) with 2% magnesium by weight and varying amounts of boron carbide particles. The fabrication process used was stir casting. The basic material chosen is an aluminum alloy, with a constant magnesium content. The reinforcement of boron carbide particles is done with varying ratios of 0%, 0.5%, 1%, 1.5%, and 2%. Carlos A. Bloem et al. [30] conducted experimental research on ternary alloys of aluminum, zinc, and magnesium, which are of increasing importance. These alloys are frequently referred to as Al-Zn-Mg. The AA7005 and AA7020 are the most often utilized aluminum alloys in this family. It has been shown that the mechanical qualities of AA7020 alloys are marginally superior to AA7005 alloys following the welding process.

A study conducted by Akbar Heidarzadeh et al. [31] examined the various FSW parameters necessary to create flawless joints in AA7020 aluminum alloy. Furthermore, a comprehensive analysis was conducted to investigate the impact of friction stir welding parameters on the tensile characteristics of the joints. In their study, Dudzik Krzysztof and Czechowski Miroslaw [32] examined the properties of 7020 and its joints welded using FSW and MIG. In their study, Reza Barenji et al. [33] examined how the speed at which the tool moves across the surface of the material affects the microstructure and mechanical properties of friction stir welded 7020-T6 aluminum alloy. The rotational speed was kept constant at 900 rpm. In their study, Marzenu Lech Grega et al. [34] conducted a quantitative examination of particle and grain size distributions in an Al-Zn-Mg (7020) alloy. The alloy was exposed to a thermal treatment that simulated the welding process.

Angadi et al. [35] examined the mechanical behavior and microstructure of a metal matrix composite consisting of Al2011 alloy reinforced with micro boron carbide particles, with the aim of assessing its suitability for aerospace applications. Their findings indicated that the inclusion of boron carbide microparticles

improved several mechanical parameters. Venkataraman et al. [36] examined the influence of carbide particles on the wear characteristics of AA2124 alloy. The wear resistance of AA2124 composites containing 9 wt.% of B<sub>4</sub>C was found to be greater.

The literature provided above indicates that there have been few or no studies conducted to investigate B<sub>4</sub>C-Al7020-based metal matrix composites (MMCs) using the stir casting technique. The Al7020-B<sub>4</sub>C composites were fabricated using an innovative two-stage stir casting technique, where the reinforcement particles were introduced into the molten metal in two separate stages. This innovative casting technique improves the wettability between the matrix and particles, hence boosting their interaction. This work aims to create and analyze metal matrix composites (MMCs) based on Al7020 reinforced with B<sub>4</sub>C.

## 2. Experimental Details

### 2.1. Materials Used

The study utilized Al7020 alloy as the matrix material and B<sub>4</sub>C as the reinforcement material. The selection of B<sub>4</sub>C as a reinforcing material was based on its exceptional characteristics, including a high melting point, remarkable hardness, low density, favorable mechanical qualities, and strong resistance to chemical assault. The chemical composition of Al7020s is provided in Table 1. Figure 1 shows the SEM of B<sub>4</sub>C particles.

**Table 1.** Chemical composition of Al7020 alloy

Elements	Weight%
Al	Balance
Si	0.35
Fe	0.40
Cu	0.20
Cr	0.10
Mg	1.10
Zn	4.20
Zr	0.10
Ti	0.25
Mn	0.40

The reinforcement (B<sub>4</sub>C) was procured from Speedfam (India) Pvt, Ltd, Ambernath, Thane, the properties of B<sub>4</sub>C are listed in Table 2.

**Table 2.** Properties of Boron Carbide

Properties	Value
Color	Black
Density (kg/m <sup>3</sup> )	2520
Melting Point (°C)	2763
Purity (%)	98
Form	Particles
Particle Size (µm)	1.10
Youngs Modulus (GPa)	450-470

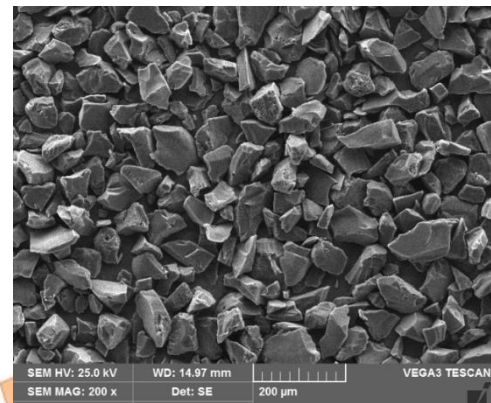


**Fig. 1.** SEM micrograph of 60-70 micron-sized B<sub>4</sub>C particles

### 2.2. Preparation of Al7020/B<sub>4</sub>C composites

Al7020-B<sub>4</sub>C composites with a particle size of 60-70 microns were made using a liquid metallurgy course and a stir-casting process. A specific amount of Al7020 compound ingots is placed in the furnace to liquefy. Aluminum alloys have a melting temperature of 660°C. The liquefy was heated to a temperature of 750 degrees Celsius. A chrome-alum thermocouple was used to record the temperature. After that, the liquid metal is degassed for 3 minutes with solid hexachloroethane (C<sub>2</sub>Cl<sub>6</sub>) [36] to remove the unwanted gases from the molten metal. To create a vortex, a tempered steel impeller coated with zirconium is used to mix the liquid metal. The stirrer will spin at 300 rpm, and the impeller will be drenched to a depth of 60 % of the liquid metal's height from the exterior of the liquefy. The Al7020-2 wt. % B<sub>4</sub>C blend is then put into a long-lasting cast-iron shape with dimensions of 120 mm in length and 15 mm in diameter. Similarly, B<sub>4</sub>C particle reinforced composites with a content of 4, 6, and 8% are manufactured and shown in Fig. 2. In addition, all the samples are machined and prepared for various mechanical tests as per the ASTM standards and shown in Fig. 3.



(a)



(e)



(b)



(c)



(d)

**Fig.2.** Castings of (a) as-cast Al7020 alloy (b) Al7020-2 wt.% B<sub>4</sub>C (c) Al7020-4 wt.% B<sub>4</sub>C (d) Al7020-6 wt.% B<sub>4</sub>C (e) Al7020-8 wt.% B<sub>4</sub>C composites



(a)



(b)



(c)

**Fig.3.** Mechanical test samples of (a) hardness (b) tensile test (c) impact test

### 2.3. Testing of specimens

The ASTM D792 [37] method is used to determine density, with standard test pieces of 12 mm in diameter and 30 mm in length. To estimate mass, the sample was soaked in distilled water at room temperature and used a numerical weighing scale with a resolution of 0.001 g. The density of a composite can be evaluated empirically with the help of a physical offset and instruments that have been calibrated in line with ASTM: D792-66.

Hardness Testing Machine VM 50 was used to conduct hardness tests (Fuel Instruments and Engineers Pvt. Ltd.). The test was carried out at the KLE Dr. M. S. Sheshgiri College of Engineering & Technology Udyambag, Belgaum, in the Mechanical Engineering Department, Material Testing Lab. The Vickers method relies on the optical measurement system as its fundamental basis. A diamond indenter is employed in the hardness test to provide a measurable indentation that can be converted into a hardness value. The Vickers Hardness test is employed to evaluate the hardness number of polished composite materials, utilizing a force of 10 kg.

**Tensile Test:** For the tensile strength test, Fuel Instruments and Engineers Pvt. Ltd.'s UNITEK-94100 universal testing machine was utilized. The exam took place at Belagavi, Karnataka, at the KLE Dr. M. S. Sheshgiri College of Engineering & Technology. Tests for tensile characteristics, such as ultimate tensile and yield strengths, are conducted on all of the prepared samples by measuring their tensile behavior.

**Compression Test:** The Universal Testing Machine TUC-400 was used to conduct the compression test on Al7020/B<sub>4</sub>C composites. The Belgaum Material Testing Centre at Udyambag, Belagavi, was the site of the test. In order to determine how a material would react when crushed, compression tests often involve applying compressive pressure to a test sample.

**Fracture Toughness Test:** The fracture toughness of the sample was determined by conducting an Izod impact test on the impact testing machine. In order to ascertain the quantity, form, and dispersion of B<sub>4</sub>C particles within Al7020 compound composites, the scanning electron microscope (TESCAN VEGA model of the Czech Republic) is employed.

## 3. Results and Discussion

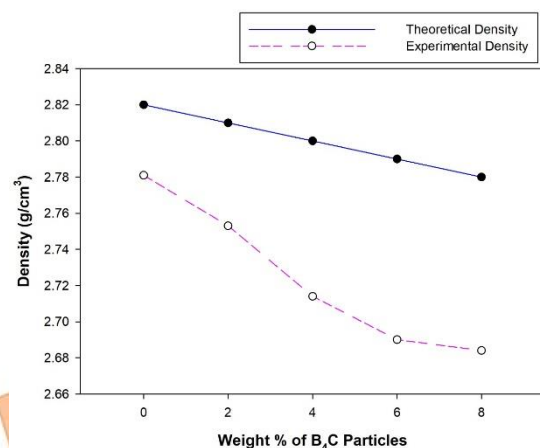
### 3.1. Density Measurements

Table 3 and Figure 4 show the densities differences between the pure Al7020, and Al7020 with 2, 4, 6, 8 wt. % B<sub>4</sub>C composites. The rule of mixture is used to compute the theoretical

density of Al7020/B<sub>4</sub>C composites. Finally, the experimental densities are calculated using the weight concept. The theoretical density of the Al7020 alloy is 2.82 g/cc, while the B<sub>4</sub>C particles only have 2.52 g/cc. Table 3 shows that the decreased density of the reinforced particles results in a lowered overall theoretical density of the composite. It should be mentioned that the actual densities are lower than what was expected. The results of these studies are consistent with those of other researchers [38, 39].

**Table 3.** Theoretical and experimental density of samples

Sl. No.	Reinforcement in wt. %	Theoretical Density (g/cc)	Experimental Density (g/cc)
1	Al7020 Alloy	2.82	2.781
2	Al7020-2% of B <sub>4</sub> C	2.81	2.753
3	Al7020-4% of B <sub>4</sub> C	2.80	2.714
4	Al7020-6% of B <sub>4</sub> C	2.79	2.690
5	Al7020-8% of B <sub>4</sub> C	2.78	2.684



**Fig. 4.** Densities of Al7020 alloy with B<sub>4</sub>C composites

### 3.2. Hardness Measurements

From zero to eight percent weight proportion of B<sub>4</sub>C particles in Al7020, the hardness grows as in Fig. 5. The VHN of pure Al7020 alloy is 81.2 VHN, while that of 2 wt. % B<sub>4</sub>C composites is 85.23 VHN, 4 wt. % 91.4 VHN 6 wt. % 95 VHN, and 8 wt. % 98.5 VHN. These values are derived from Figure 5 and Table 4. The existence of solid B<sub>4</sub>C particles is attributed to contributing to the improved hardness by impeding the mobility of dislocations inside the Al alloy matrix. The strain energy around the microparticles is raised

following their addition, leading to greater hardness in composites [40, 41].

**Table 4.** The hardness of Al7020-B<sub>4</sub>C composites

Sl. No.	Material	Hardness (VHN) with Standard Deviation
1	Al7020 Alloy	81.20 ± 1.05
2	Al7020 – 2 % of B <sub>4</sub> C	85.23 ± 1.10
3	Al7020 – 4 % of B <sub>4</sub> C	91.46 ± 1.15
4	Al7020 – 6 % of B <sub>4</sub> C	95.06 ± 0.92
5	Al7020 – 8 % of B <sub>4</sub> C	98.50 ± 0.66

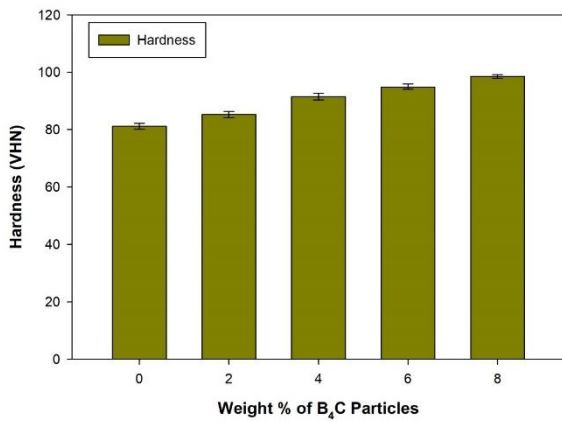


**Fig.5.** Hardness of Al7020 Alloy with B<sub>4</sub>C Composites

This morphology is observed in the microstructures as maximum B<sub>4</sub>C particles spread over the Al7020 matrix, strengthening the composite bonding behavior [42]. Similarly, the B<sub>4</sub>C is spotted as having better dispersion in the Al matrix and resists the indentation without dislocation of particle movements. Most of the B<sub>4</sub>C particle is well dispersed in the Al phase offering better output performance during the evaluation of mechanical properties of composites.

### 3.3. Tensile Properties

Tensile properties such as ultimate, yield strength, and % elongation are evaluated by conducting tensile tests on cast Al7020 alloy and Al7020 alloy with 2 to 8 weight percentages of B<sub>4</sub>C as in Tables 5, 6, and 7 and Fig. 6, 7, and 8.

Al7020/B<sub>4</sub>C MMCs' ultimate and yield strengths were affected by B<sub>4</sub>C particles, as shown in Fig. 6 and 7. The UTS and yield strength of MMCs have been enhanced by the addition of B<sub>4</sub>C. Both the ultimate tensile strength (298.12 MPa) and the yield strength (272.13 MPa) of Al7020 alloy with 8 weight percent B<sub>4</sub>C particles are the highest values. When the amount of B<sub>4</sub>C in Al7020 grows from 0% to 8% by weight, the alloy's strength increases even more. By increasing UTS, interface bonding shifts the stress away from the matrix and onto the

reinforcements. Numerous researchers have made similar findings in various studies [43, 44].

**Table 5.** Ultimate tensile strength of Al7020-B<sub>4</sub>C composites

Sl. No.	Material	Ultimate Tensile Strength (MPa) with Standard Deviation
1	Al7020 Alloy	195.13 ± 1.06
2	Al7020 – 2 wt.% of B <sub>4</sub> C	211.06 ± 1.39
3	Al7020 – 4 wt.% of B <sub>4</sub> C	254.16 ± 1.12
4	Al7020 – 6 wt.% of B <sub>4</sub> C	271.63 ± 1.04
5	Al7020 – 8 wt.% of B <sub>4</sub> C	298.16 ± 1.47

The un-reinforced alloy records an ultimate strength of 195.13 MPa these are the lowest values as compared to the micro B<sub>4</sub>C reinforced Al7020 composites. 8 wt. % of B<sub>4</sub>C filled composites record a maximum ultimate strength of 298.16 MPa. This confirms the improvement in tensile strength as the addition of micro B<sub>4</sub>C increases. 8 wt. % of carbide particles filled composite shows improvement of ultimate strength of 52.8% as compared to as-cast Al alloy. The addition of microparticles to Al matrix composites has increased their tensile strength because these particles are more rigid than the matrix [45]. Several researchers have also confirmed that adding filler to the composite improves its tensile qualities [46]. The enhanced tensile properties may be attributed to the superior particle or fiber quality, strong interfacial adhesion between the reinforcements and matrix, and minimal vacancy fraction values.

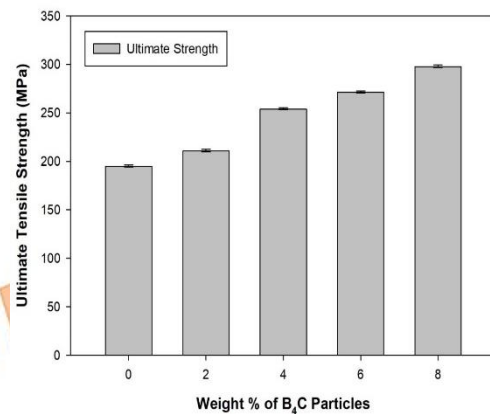


**Fig. 6.** Ultimate Strength of Al7020 Alloy with B<sub>4</sub>C Composites

Previous research on Al/B<sub>4</sub>C composites has also corroborated this. Furthermore, B<sub>4</sub>C is a rigid ceramic material with a substantial modulus of 425 GPa. Figure 11 (b-c) shows that the B<sub>4</sub>C particles are evenly distributed throughout the Al7020 matrix, which enhances the load-bearing capacity of the matrix. The lack of cracks in the vicinity of the Al – B<sub>4</sub>C contact enhances the strength of the interface, promoting the load-

bearing capacity and therefore enhancing the ultimate tensile strength (UTS) and yield strength (YS). Decreasing the size of the grains in composites leads to an increase in the amount of grain boundaries, which in turn limits the movement of dislocations. This restriction contributes to the enhancement of the ultimate tensile strength (UTS). Orowan Strengthening does not have a prominent role in micron-sized reinforced Metal Matrix Composites (MMCs).

**Table 6.** Yield strength of Al7020-B<sub>4</sub>C composites

Sl. No.	Material	Yield Strength (MPa) with Standard Deviation
1	Al7020 Alloy	154.70 ± 0.85
2	Al7020 – 2 % of B <sub>4</sub> C	166.53 ± 0.87
3	Al7020 – 4 % of B <sub>4</sub> C	199.50 ± 1.15
4	Al7020 – 6 % of B <sub>4</sub> C	213.40 ± 1.15
5	Al7020 – 8 % of B <sub>4</sub> C	272.06 ± 1.55

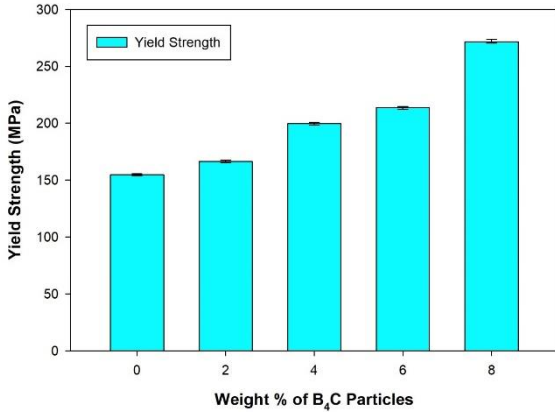


**Fig. 7.** Yield strength of Al7020 Alloy with B<sub>4</sub>C Composites

**Table 7.** Elongation of Al7020-B<sub>4</sub>C composites

Sl. No.	Material	Elongation (%) with Standard Deviation
1	Al7020 Alloy	11.26 ± 0.07
2	Al7020 – 2 % of B <sub>4</sub> C	10.10 ± 0.10
3	Al7020 – 4 % of B <sub>4</sub> C	9.08 ± 0.07
4	Al7020 – 6 % of B <sub>4</sub> C	7.73 ± 0.08
5	Al7020 – 8 % of B <sub>4</sub> C	7.18 ± 0.07

The % of elongation of the Al matrix decreases slightly as the weight % of particles in the matrix increases. The ductility of Al7020-B<sub>4</sub>C composites decreases as the wt. % of boron carbide particles increases from 2% to 8%, mainly due to the brittleness of hard reinforcement particles, which in turn decreases in ductility and % of elongation which is shown in Fig. 8.

### 3.4. Impact and Compression strength

**Table 8.** Fracture strength of Al7020-B<sub>4</sub>C composites

Sl. No.	Material	Fracture Strength (J) with Standard Deviation
1	Al7020 Alloy	6.82 ± 0.12
2	Al7020 – 2 wt.% of B <sub>4</sub> C	3.78 ± 0.10
3	Al7020 – 4 wt.% of B <sub>4</sub> C	2.85 ± 0.06
4	Al7020 – 6 wt.% of B <sub>4</sub> C	1.91 ± 0.07
5	Al7020 – 8 wt.% of B <sub>4</sub> C	1.24 ± 0.08

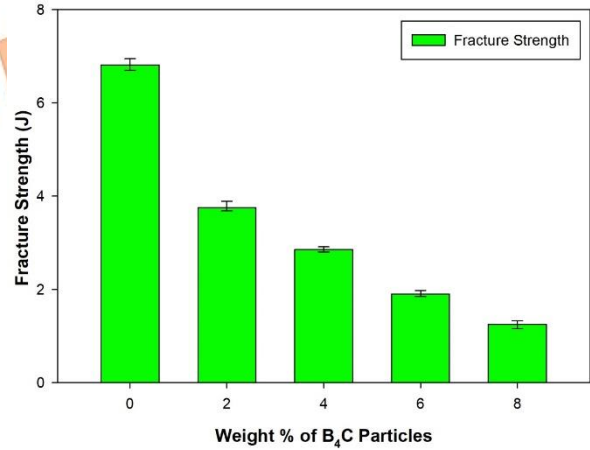


**Fig. 9.** Fracture strength of Al7020 Alloy with B<sub>4</sub>C Composites

The fracture strength of Al7020/B<sub>4</sub>C decreases as the weight % of boron carbide increases in the composite. As indicated in Fig. 9 addition of B<sub>4</sub>C particles decreases the fracture strength, it is mainly due to particle agglomeration and incompatibility between B<sub>4</sub>C and aluminum.

**Table 9.** Compression strength of Al7020-B<sub>4</sub>C composites

Sl. No.	Material	Compression Strength (MPa) with Standard Deviation
1	Al7020 Alloy	633.25 ± 7.92
2	Al7020 – 2 % of B <sub>4</sub> C	865.26 ± 5.58
3	Al7020 – 4 % of B <sub>4</sub> C	894.06 ± 3.29
4	Al7020 – 6 % of B <sub>4</sub> C	914.85 ± 4.23
5	Al7020 – 8 % of B <sub>4</sub> C	951.71 ± 3.95

In Fig. 10, we can see the compression strength of composites reinforced with micron B<sub>4</sub>C particles and based on Al7020 alloy. With the addition of B<sub>4</sub>C particles, the Al7020 alloy's compression strength has been enhanced. The enhanced compression strength is mainly attributable to the B<sub>4</sub>C hard ceramic particles embedded in the soft matrix. The strength gain is credited to the real interaction between the matrix and reinforcing components. The strength and quality of composites are improved by stronger grain boundaries, this can be a result of the reinforcement's load transfer mechanism to the matrix, which strengthens the structure. The

dispersion of tough ceramic particles is another factor contributing to the increase in strength.

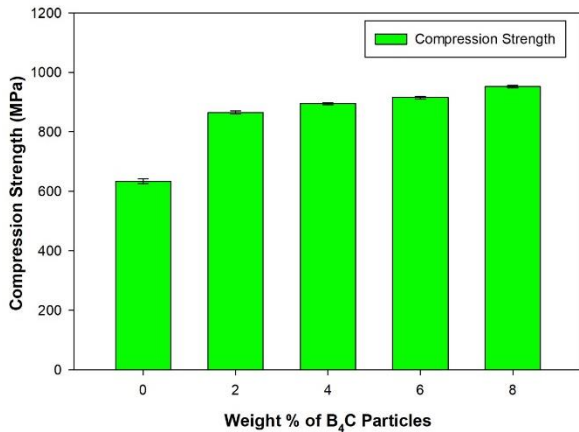
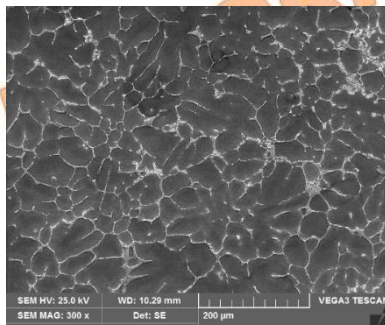


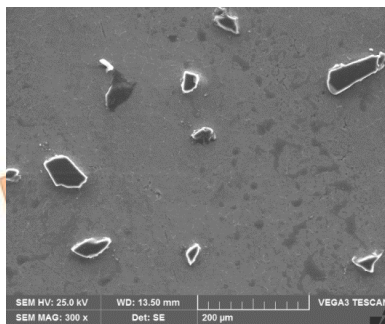
**Fig. 10.** Compression strength of Al7020 Alloy with B<sub>4</sub>C Composites

### 3.5. Microstructural study

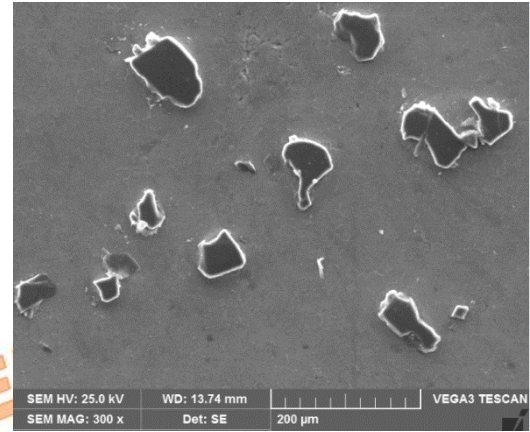
Microstructural analysis of prepared samples has been carried out by using SEM. Figure 11 (a-c) shows SEM images of pure Al7020 alloy and micro B<sub>4</sub>C reinforced composites. Figure 11 (a) shows the SEM of a pure Al7020 alloy. Figure 11 (b-c) shows micrographs of Al7020 with 2, 4, 6, and 8 wt. % of B<sub>4</sub>C composites. From the micrograph, it is clear that the reinforcement particles are uniformly distributed throughout the aluminum matrix material.



(a)

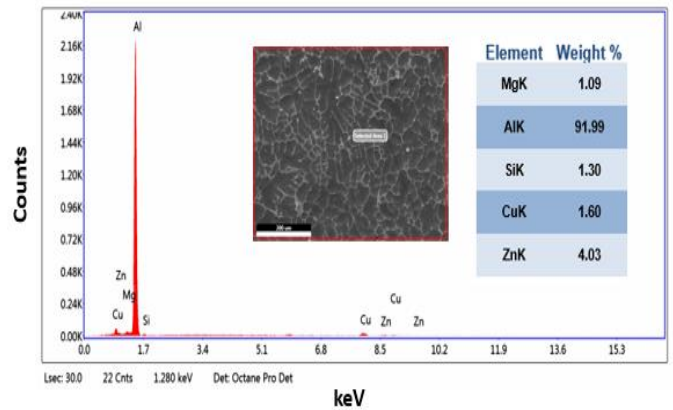


(b)

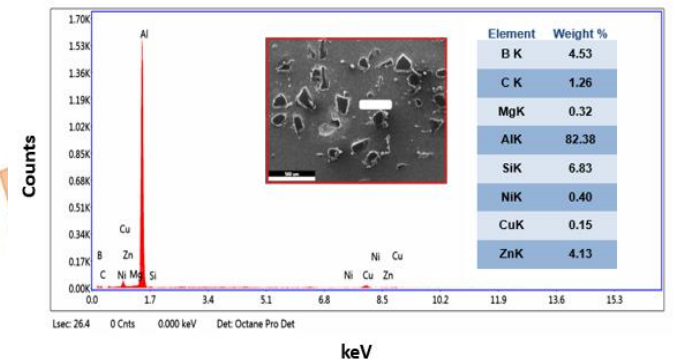


(c)

**Fig. 11.** SEM images of (a) Al7020 alloy (b) Al7020-4% B<sub>4</sub>C (c) Al7020-8% B<sub>4</sub>C composites



(a)



(b)

**Fig. 12.** EDS spectrums of (a) Al7020 alloy (b) Al7020-8% B<sub>4</sub>C composite

In Fig.11 (a-c) and Fig. 12 (a-b), the distribution of B<sub>4</sub>C particles within the Al7020 matrix is revealed by the SEM-EDS elemental mapping analysis. The mapping study revealed that the matrix has a well-distributed distribution of tiny particles, specifically B<sub>4</sub>C



particles. It is impossible to exaggerate the significance of this equitable distribution. The first benefit is an improvement to the composite's mechanical properties brought about by optimized load transfer between the matrix and the reinforcing particles. The development of particle clusters or agglomerates that might result in stress concentration and potential failure points is also reduced. To achieve improved mechanical characteristics, like, escalated strength and hardness, a uniform dispersion is essential.

The SEM-EDS elemental mapping analysis for Fig.11b-c and Fig. 12b is concentrated on the dispersion of B<sub>4</sub>C particles within the Al7020 matrix. The mapping analysis reveals a fine particle distribution that is excellent, with carbide particles evenly distributed throughout the matrix. The multitude of merits result from the particles' uniform distribution. Firstly, having particles in the composite makes it more thermally conductive. Secondly, the B<sub>4</sub>C particle distribution enhances the composite's stiffness and strength. By quantifying the elemental composition, the EDS analysis supports the excellent fine particle distribution observed in the mapping analysis and ensures that carbide particles are present in the matrix in the desired proportions and distributed uniformly.

#### 4. Conclusions

The current study involved the fabrication of Al7020 alloy and Al7020/B<sub>4</sub>C MMCs using the stir casting method, with different weight percentages of B<sub>4</sub>C. An assessment was conducted on the physical, mechanical properties, and microstructure of the MMCs. The present analysis and review yielded the following significant conclusions.

- Composites made of Al7020 alloy with 2 to 8 weight percent micro-sized B<sub>4</sub>C particles for reinforcement have been effectively produced using the stir casting process.
- SEM micrographs show a very uniform distribution of 4 and 8 wt. % of B<sub>4</sub>C particles throughout the Al7020 alloy.
- EDS spectrums confirmed the existence of boron carbide particles in the Al7020 alloy composites.
- The Theoretical and experimental density of samples decreases as the wt. % of B<sub>4</sub>C particles increases in the composites.
- The hardness of the Al7020 alloy rose in direct proportion to the weight percentage of B<sub>4</sub>C. Al7020-8 weight percent of B<sub>4</sub>C composites has a

hardness of 98.5 VHN, while the as-cast Al7020 alloy has a hardness of 81.23 VHN. The hardness of Al7020 alloy improved by 21.3% when 8 wt. % B<sub>4</sub>C composites were added.

- The ultimate and yield strengths of the Al7020 material are enhanced by adding B<sub>4</sub>C particles. The addition of 8-weight percent boron carbide particles to the Al7020 alloy provides a 52.8% increase in ultimate strength. The Al7020 - 8 wt.% boron carbide composites show an improvement of about 75.8%.

- A small decrease in the elongation of the Al matrix is observed when the weight wt.% of hard particles in the matrix increases.

- Adding hard boron carbide particles to the Al7020 alloy reduced its impact strength.

- With the addition of B<sub>4</sub>C particles, the Al7020 alloy's compression strength has been enhanced. The as-cast Al7020 alloy has a compression strength of 633.25 MPa, and when combined with 8 weight percent B<sub>4</sub>C composites, it exhibits an improvement of approximately 50.29 percent.

- The fracture strength of Al7020/B<sub>4</sub>C decreases as the weight % of boron carbide increases in the composite.

- Al7020 alloy is widely used in aerospace structural applications. In the present work, Al7020 with 8 wt. % exhibited an improvement of 52.8% in the ultimate strength, hence these metal composites can be used for wing root fittings and bulk-heads of aircraft structural components with reduced cross-sectional to save the weight of the product.

#### Conflicts of Interest

The author declares that there is no conflict of interest regarding the publication of this article.

#### References

- [1] Ali, K.S.A., Mohanavel, V., Vendan, S.A., Ravichandran, M., Yadav, M.A., Gucwa, J. W., 2021. Mechanical and microstructural characterization of friction stir welded SiC and B<sub>4</sub>C reinforced aluminum alloy AA6061 metal matrix composites. *Materials (Basel)* 14, 3110.
- [2] Ramanathan, A., Krishnan, P.K., Muraliraja, R., 2019. A review on the production of metal

- matrix composites through stir casting—furnace design, properties, challenges, and research opportunities. *Journal of Manufacturing Process*, 42, pp. 213–245.
- [3] Yang, M., Li, Y.C., Zhang, D., Jia, R., Li, Hou, Y., Cao, J.H., 2019. Predictive model for minimum chip thickness and size effect in single diamond grain grinding of zirconia ceramics under different lubricating conditions. *Ceramic International*, 45, pp.14908–14920.
- [4] Kumar, A., Kumar, S., Mukhopadhyay, N.K., Yadav, A., Kumar, V., Winczek, J., 2021. Effect of variation of SiC reinforcement on wear behaviour of AZ91 alloy composites. *Materials (Basel)*, 14, 990.
- [5] Kumar, A., Kumar, S., Mukhopadhyay, N.K., Yadav, A., Winczek, J., 2020. Effect of SiC reinforcement and its variation on the mechanical characteristics of AZ91 composites. *Materials (Basel)*, 13, 4913.
- [6] Yang, M., Li, C., Zhang, Y., Jia, D., Zhang, X., Hou, Y., Li, R., Wang, J., 2017. Maximum undeformed equivalent chip thickness for ductile-brittle transition of zirconia ceramics under different lubrication conditions. *International Journal of Machine Tools and Manufacturing*, 122, pp. 55–65.
- [7] Gao, T., Li, C., Yang, M., Zhang, Y., Jia, D., Ding, W., Debnath, S., Yu, T., Said, Z., JWang, J., 2021. Mechanics analysis and predictive force models for the single-diamond grain grinding of carbon fiber reinforced polymers using CNT nano-lubricant. *Journal of Materials Processing Technology*, 290, 116976.
- [8] Pazhouhanfar, Y., Eghbali, B., 2018. Microstructural characterization and mechanical properties of TiB<sub>2</sub> reinforced Al6061 matrix composites produced using stir casting process. *Materials Science and Engineering A*, 710, pp. 172–180.
- [9] Madeva, N., Auradi, V., Kori, S.A., 2015. Microstructure and mechanical properties of Al6061-Graphite composites fabricated by stir casting process. *Applied Mechanics and Materials*, 766, pp. 308-314.
- [10] Senthil Kumar, P., Kavimani, V., Soorya Prakash, K., Murali Krishna, V., Shanthos Kumar, G., 2019. Effect of TiB<sub>2</sub> on the corrosion resistance behavior of In Situ Al composites. *International Journal of Metalcasting*, 14, pp. 84–91.
- [11] Madeva, N., Vijaykumar, H., Auradi, V., Kori, S.A., 2018. Influence of Two-Stage Stir Casting Process on Mechanical Characterization and Wear Behavior of AA2014-ZrO<sub>2</sub> Nano-composites, *Transactions of the Indian Institute of Metals*, 71, pp. 2845-2850.
- [12] Shinde, D.M., Sahoo, P., 2022. Influence of speed and sliding distance on the tribological performance of submicron particulate reinforced Al-12Si/1.5 wt% B<sub>4</sub>C composite. *International Journal of Metalcasting*, 16, pp. 739-758..
- [13] Pathalinga, G.P., Chittappa, H.C., Madeva, N., Auradi, V., 2020. Influence of B<sub>4</sub>C Reinforcement Particles with Varying Sizes on the Tensile Failure and Fractography of LM29 Alloy Composites. *Journal of Failure Analysis and Prevention*, 20 (6), pp. 2078-2086.
- [14] Jayasheel, I.H., Prasad, T.B., Madeva, N., Pankaj, J., Auradi, V., 2017. Microstructure and dry sliding wear behaviour of Al2219-TiC composites. *Materials Today: Proceedings*, 4 (10), pp. 11004-11009
- [15] Bharath, V., Auradi, V., Madeva, N., Satish, B.B., Ramesh, S., Palanikumar, K., 2021. Microstructural and wear behavior of Al2014-alumina composites with varying alumina content. *Transactions of the Indian Institute of Metals*, 75, pp. 133-147.
- [16] Madeva, N., Auradi, V., Kori, S.A., Veena, S., 2020. Mechanical characterization and wear behavior of nano TiO<sub>2</sub> particulates reinforced Al7075 alloy composites. *Mechanics of Advanced Composite Structures*, 7(1), pp. 71-78.
- [17] Ajay Kumar, P., Rohatgi, P., Weiss, D., 2019. 50 years of foundry-produced metal matrix composites and future opportunities. *International Journal of Metalcasting*, 14, pp. 291–317.
- [18] Zeeshan, A., Muthuraman, V., Rathnakumar, P., Gurusamy, P., Madeva, N., 2022. Studies on mechanical properties of 3 wt% of 40 and 90 μm size B<sub>4</sub>C particulates reinforced A356 alloy composites. *Materials Today: Proceedings*, 52, pp. 494-499.
- [19] Raj, K., Deshpande, R.G., Gopinath, B., Jayasheel, H., Nagaral, M., Auradi, V., 2021. Mechanical Fractography and Worn Surface Analysis of Nanographite and ZrO<sub>2</sub>-Reinforced Al7075 Alloy Aerospace Metal Composites, *Journal of Failure Analysis and Prevention*, 21, pp. 525-536.
- [20] Bharath, V., Santhrusht, S.A., Nagaral, M., Auradi, V., Kori, S.A., 2019. Characterization and Mechanical Properties of 2014 Aluminum Alloy Reinforced with Al<sub>2</sub>O<sub>3</sub>p

- Composite Produced by Two-Stage Stir Casting Route. *Journal of The Institution of Engineers (India): Series C*, 100, pp. 277-282.
- [21] Kumar, V.A., Anil, M.P., Rajesh, G.L., Hiremath, V., Auradi, V., 2018. Tensile and compression behaviour of boron carbide reinforced 6061Al MMC's processed through conventional melt stirring. *Materials Today Proceedings*, 5, pp.16141-16145.
- [22] Satheesh, M., Pugazhvadivu, M., 2019. Investigation on physical and mechanical properties of Al6061-silicon carbide (SiC)/coconut shell ash (CSA) hybrid composites. *Phys. B Condens. Matter*. 572, pp.70-75.
- [23] Madeva, N., Auradi, V., Parashivamurthy, K.I., Kori, S.A., Shivananda, B.K., 2018. Synthesis and characterization of Al6061-SiC-graphite composites fabricated by liquid metallurgy. *Materials Today: Proceedings*, 5(1), pp. 2836-2843.
- [24] Atabak, R., 2018. Laboratory Research on Effect of Friction Stir Processing. *International Journal of Advances in Science Engineering and Technology*, 6 (1), pp. 2321-8991.
- [25] Zeeshan, A., Muthuraman, V., Rathnakumar, P., Gurusamy, P., Nagaral, M., 2020. Investigation on the tribological properties of copper alloy reinforced with Gr/ZrO<sub>2</sub> particulates by stir casting route. *Materials Today: Proceedings*, 33, pp. 3449-3453.
- [26] Akbar, H., Reza, V.B., Barenji, M.E., Atabak, R.I., 2015. Tensile Properties of Friction Stir Welds of AA 7020 Aluminum alloy. *Transactions of the Indian Institute of Metals*, 68, pp. 757-767.
- [27] Samuel, D., Satish, B.B., Auradi, V., Nagaral, M., Udaya M.R., Bharath, V., 2021. Evaluation of Wear Properties of Heat-Treated Al-ALB2 in-situ Metal Matrix Composites. *Journal of Bio-and Tribo-Corrosion*, 7, 40, pp. 1-11
- [28] Cun-Zhu, N., Jia-Jun, G., Jun-Liang, L., Zhang, D., 2007. Production of Boron Carbide Reinforced 2024 Aluminum Matrix Composites by Mechanical Alloying. *Materials Transactions*, 48 (5), pp. 990- 995.
- [29] Chaitra, H.M., Ghanaraja, S., Srinivasa, M.R., 2021. Analysis on Characterization of Aluminum 7075 Reinforced with Magnesium and Boron Carbide. *International Journal of Engineering Research in Electronics and Communication Engineering*, 8(8).
- [30] Carlos, B., Maria, S., Vicente, A., Mary, V., 2011. Aluminum 7020 Alloy and Its Welding Fatigue Behaviour. *Aluminum Alloys, Theory and Applications*.
- [31] Akbar, H., Reza, V., Barenji, V., Mohsen, E., Atabak, R.I., 2015. Rahimzadeh Ilkhichi. Tensile Properties of Friction Stir Welds of AA 7020 Aluminum Alloy. *Transactions of Indian Institute of Metals*, 68(5), pp.757-767.
- [32] Dudzik, K., Czechowski, M., 2015. Influence of Joining Method for Mechanical Properties Of 7020 Aluminum Alloy Joints. *Diffusion and Defect Data Pt. B: Solid State Phenomena*, 220-221, pp.583-588.
- [33] Reza, V.B., 2015. Effect of tool traverse speed on microstructure and mechanical performance of friction stir welded 7020 aluminum alloy. April 2015. *Proceedings of the Institution of Mechanical Engineers Part L Journal of Materials Design and Applications*, 230(2).
- [34] Marzena, L.G., Sonia, H.C, Maria, R., Wojciech, S., 2001. Structural parameters of 7020 alloy after heat treatment simulating the welding process. *Materials Characterization*, 46(2), pp.251-257.
- [35] Angadi, S.B., Nagaral, M., Pilankar, V., Yarnalkar, P., Purohit, B., Shewale, S., 2023. Assessment of Mechanical Behaviour and Microstructure of Micro Boron Carbide Particles Reinforced Al2011 Alloy Metal Matrix Composite for Aerospace Applications. *International Journal of Vehicle Structures & Systems*, 15(2), pp. 251-257.
- [36] Venkataraman, V., Nagaral, M., 2020. Mechanical characterization and wear behavior of aerospace alloy AA2124 and micro B4C reinforced metal composites. *Journal of Metals, Materials and Minerals*, 30, 4, pp. 97-105.
- [37] Nagaraj, N., Mahendra, K.V., Nagaral, M., 2018. Microstructure and evaluation of mechanical properties of Al-7Si-fly ash composites. *Materials Today: Proceedings*, 5 (1), pp. 3109-3116.
- [38] Mithun, B.R., Nagaral, M., Auradi, V., Bharath, V., 2017. Microstructure and mechanical properties of Cu coated Al2O3 particulate reinforced 6061 Al metal matrix composites. *Materials Today Proceedings*, 4 (10), pp. 11015-11022.
- [39] Vasanth, K.H.S., Revanna, K., Nithin, K., Sathyanarayana, N., Madeva, N., Manjunath, G.A., Adisu, H., 2022. Impact of Silicon Carbide Particles Weight Percentage on the Microstructure, Mechanical Behaviour, and

- Fractography of Al2014 Alloy Composites. *Advances in Materials Science and Engineering*, 2839150.
- [40] Madeva, N., Shivananda, B.K., Auradi, V., Kori, S.A., 2020. Development and mechanical-wear characterization of Al2024-nano B 4C composites for aerospace applications. *Strength, Fracture and Complexity*, 13 (1), pp. 1-13.
- [41] Krishna, D., Prashanth, L., Nagaral, M., Rakesh, M., Hanumantharayagouda, M.B., 2017. Microstructure and mechanical behavior of B<sub>4</sub>C particulates reinforced ZA27 alloy composites. *Materials Today: Proceedings*, 4 (8), pp. 7546-7553.
- [42] Balaraj, V., Nagaraj, K., Nagaral, M., Auradi, V., 2021. Microstructural evolution and mechanical characterization of micro Al<sub>2</sub>O<sub>3</sub> particles reinforced Al6061 alloy metal composites. *Materials Today: Proceedings*, 47, pp. 5959-5965.
- [43] Bharath, V., Auradi, V., Nagaral, M., 2021. Fractographic characterization of Al203p particulates reinforced Al2014 alloy composites subjected to tensile loading. *Frattura ed Integrità Strutturale*, 15(57), pp. 14-23.
- [44] Nagaraj, N., Mahendra, K.V., Nagaral, M., 2018. Investigations on mechanical behaviour of micro graphite particulates reinforced Al-7Si alloy composites. *IOP Conference Series: Materials Science and Engineering*, 310 (1), 012131.
- [45] Rashmi, P.S., Mahesh, T.S., Zeeshan, A., Veeresha, G., Nagaral, M., 2022. Studies on mechanical behaviour and tensile fractography of boron carbide particles reinforced Al8081 alloy advanced metal composites. *Materials Today: Proceedings*, 52, pp. 2115-2120.
- [46] Nagaral, M., Auradi, V., Bharath, B., 2022. Mechanical characterization and fractography of 100 micron sized silicon carbide particles reinforced Al6061 alloy composites, *Metallurgical and Materials Engineering*, 28 (1), pp. 17-32.

UNCORRECTED PROOF

UNCORRECTED PROOF